JCTC Journal of Chemical Theory and Computation

ARTICLE

pubs.acs.org/JCTC

Unraveling the Molecular Mechanism of Enthalpy Driven Peptide Folding by Polyol Osmolytes

Regina Gilman-Politi and Daniel Harries*

Institute of Chemistry and The Fritz Haber Center, The Hebrew University, Jerusalem 91904, Israel

Supporting Information

ABSTRACT: Many polyols and carbohydrates serve in different organisms as protective osmolytes that help to stabilize proteins in their native, functional state, even under a variety of environmental stresses. However, despite their important role, much of the molecular mechanism by which these osmolytes exert their action remains elusive. We have recently shown experimentally that, although polyols and carbohydrates are excluded from protein and peptide interfaces, as also expected for the known entropic "crowding" mechanism, the osmolyte folding action can in fact primarily be enthalpic in nature. To follow this newly resolved enthalpically driven stabilization mechanism, we report here on molecular dynamics simulations of a model peptide that can fold in solution into a β-hairpin. In agreement with experiments, our simulations indicate that sorbitol, a representative polyol, promotes peptide folding by preferential exclusion. At the molecular level, simulations further show that peptide stabilization can be explained by sorbitol's perturbation of the solution hydrogen bonding network in the peptide first hydration shells. Consequently, fewer hydrogen bonds between peptide and solvating water are lost upon folding, and additional internal peptide hydrogen bonds are formed in the presence of sorbitol, while internal peptide and water-associated hydrogen bonds are strengthened, resulting in stabilization of the peptide folded state. We further find that changes in water orientational entropy are reduced upon folding in sorbitol solution, reflecting the struggle of water molecules to maintain optimal hydrogen bonding in the presence of competing polyols. By providing first molecular underpinnings for enthalpically driven osmolyte stabilization of peptides and proteins, this mechanism should allow a better understanding of the variety of physical forces by which protective osmolytes act in biologically realistic solutions.

INTRODUCTION

Protein stability and activity sensitively depend on myriad modulators of environmental solvent conditions, including hydration levels, ion concentrations, and pH. In efforts to maintain protein function and integrity, one of the important ways that living organisms combat such environmental stresses involves the accumulation of molecularly small cosolutes termed osmolytes.[1−3] Naturally occurring osmolytes are cosolutes that can be typically grouped into three major classes: polyols, amino acids, and combinations of methylamines with urea.[1] Of these, the addition of "protective" osmolytes to protein solutions shifts the thermodynamic equilibrium of folding toward more compact, native states. While protein folding by osmolytes has been a subject of numerous investigations,[4−13] much of the underlying molecular mechanism remains unknown.

Protective osmolytes are generally excluded from protein−water interfaces, and it is this preferential exclusion from macromolecular surfaces that necessarily confers thermodynamic stability to proteins.[10,14−20] Molecular crowding due to excluded volume interactions has been widely invoked to explain how osmolytes can shift the folding equilibrium toward the more folded state.[21−25] According to this mechanism, the restriction of protein conformations to allow larger free volume for the added osmolytes destabilizes the unfolded state with respect to the native conformation.[23,26] Crowding has been useful in explaining the protein stabilizing effect of macromolecular solutes, such as polymers and other proteins, based on steric interactions that are entropic in nature.[27−30]

In contrast to entropically driven steric "crowding", recent evidence indicates that, when molecularly small solutes are involved, the stabilizing mechanism may be enthalpically dominated.[31,32] For example, our recent experiments indicate that sugars and polyols can drive peptide folding primarily through diminishing the enthalpic loss involved in the folding process. Moreover, the added entropic contribution to folding wrought by osmolytes is negative, and disfavors folding. Interestingly, these effects are dependent on the molecular size of the osmolytes, as also expected for a crowding mechanism. These findings require new molecular mechanisms that can explain how osmolytes can confer a favorable enthalpic contribution to folding, while concurrently remaining preferentially excluded from the peptide−solution interface.

Here, we employ molecular dynamics (MD) simulations to explore the molecular origins of the stabilizing mechanism of protective osmolytes. We follow a model 16-residue peptide that has been shown experimentally to fold into a β-hairpin from a disordered state.[32,33] At room temperature and pH 7, about half of the peptide population is found in the folded state ($\Delta G_{fold} \approx 0$). In the presence of polyols and carbohydrates, however, the equilibrium is shifted, and the peptide primarily adopts the folded state. Our strategy was to separately simulate the folded and unfolded states of the peptide in two different solvating solutions: pure water and aqueous solutions of osmolyte. We focus on

Received: June 30, 2011
Published: September 22, 2011

sorbitol as an important representative of polyol osmolytes; sorbitol is one of the largest polyols, is highly soluble, and has been experimentally shown to have one of the strongest effects on peptide folding in this group. Because the sorbitol and water translational and orientational relaxation around the peptide (on the order of hundreds of picoseconds) is much faster than the peptide folding−unfolding times (estimated at several hundreds of nanoseconds), we have been able to exploit this difference in time scales to separately average the properties of solution microstates around the folded and unfolded populations.

By analyzing the changes in the solvating environment of the folded and unfolded states in the presence of osmolytes, and comparing these to the differences in pure water found around both states, we characterized a previously unknown enthalpy driven mechanism for polyol stabilization of peptides. Our results reveal that the key driving forces for peptide stabilization by osmolytes involve the reduced loss upon folding of the number of hydrogen bonds located in the first and second solvation layers around the peptide, the increased strength of the hydrogen bonds that remain, and the larger number of internal peptide hydrogen bonds created in the presence of the polyol.

RESULTS

Changes in the model peptide's secondary structure in both water and sorbitol solution (at 3.9 Osm) can be followed by tracking the solvent accessible surface area (ASA) for the folded (F) and unfolded (U) states over the MD trajectory, as shown in Figure 1 and detailed in the Methods. The U state undergoes larger fluctuations in ASA than the F state (with a standard deviation of 78 vs 68 Å^2 in pure water, and 95 vs 59 Å^2 in sorbitol solution, respectively); however, on the basis of average ASA alone, there is no discernible difference between the U states in water and in the presence of sorbitol. Similarly, the F state also showed no significant difference in ASA for the first 30 ns simulated, but at longer times we find more compact structures in the presence of sorbitol than in pure water (smaller ASA by, on average, 100 Å^2 over the last 20 ns). While these observations already qualitatively match the known peptide stabilizing capacity of sorbitol, additional thermodynamic measures can provide a direct link between solvation thermodynamics and sorbitol-induced peptide stability, as we discuss in the following sections.

Sorbitol is Preferentially Excluded from Peptide Interfaces. In general, stabilizing cosolutes are found to be "excluded" from the macromolecular peptide interfaces and thereby increase the chemical potential of the macromolecule; in the limit of infinite peptide dilution, this necessarily also implies that the peptide is "preferentially hydrated".[19] To assess osmolyte exclusion as well as the distance and size of different solvation layers around the peptide in the F and U states, we follow the structure of solution using the radial distribution function, $g_{Px}(r)$, representing the local densities with respect to the bulk of species x at a distance r from the peptide (P), where x represents the chemical species in solution: peptide (P), solute (S), or water (W) (see also Methods). Figure 2a shows $g_{PW}(r)$ and $g_{PS}(r)$ for the local densities of water's oxygen and sorbitol's center of mass, respectively, where r represents the shortest distance from *any atom* of the folded peptide states.

In contrast to the results often reported for proteins using MD simulations and neutron diffraction experiments,[34,35] the peptide−water distribution function $g_{PW}(r)$ shows not one, but two prominent hydration peaks, Figure 2a. This apparent discrepancy

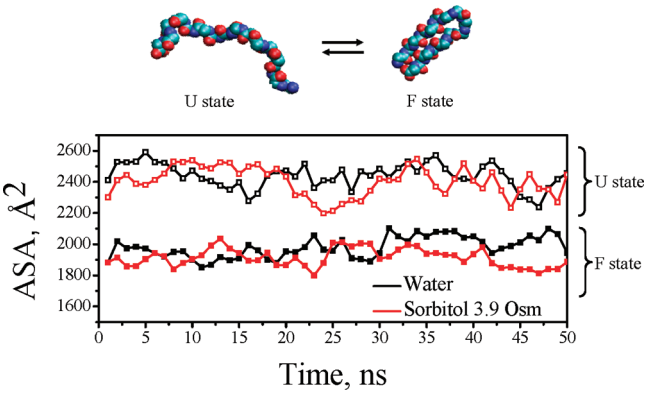

Figure 1. Solvent accessible surface area (ASA) calculated over 50 ns of MD simulation for the peptide folded (F) and unfolded (U) states in pure water (black line) and in the presence of sorbitol aqueous solutions at a concentration of 3.9 Osm (red line). Each data point represents an average ASA taken over the course of 1 ns. The upper panel shows a schematic of the F and U states.

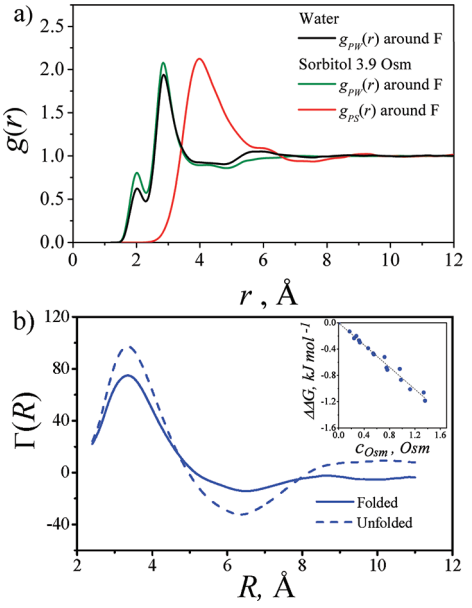

Figure 2. Solution structure around the folded state and preferential interaction coefficients for the folded and unfolded states. (a) Radial distribution function, $g(r)$, of water oxygen's and sorbitol's centers of mass around the peptide. (b) Preferential interaction coefficient, Γ, of water near the peptide. The inset in b shows experimental data for the folding free energy versus sorbitol's osmolyte concentration at T = 298 K, reproduced from ref 32. Both $g(r)$ and $\Gamma(R)$ are plotted versus the distance from any peptide atom.

results from the way we calculate $g(r)$: here, distances are measured with respect to each peptide atom, rather than from a single point (such as the peptide center of mass) that tends to smear out these two hydration peaks. The first peak in $g_{PW}(r)$, representing the first hydration layer, appears at $r \approx 2$ Å and is mainly associated with water molecules localized close to the charged amino acid Lys, as well as Asn, Ser, and Thr, which show the largest average number of neighboring water molecules within this first hydration layer, see Supporting Information Figure S2. These water molecules primarily orient with oxygen toward the

peptide, Supporting Information Figure 3S. The second peak in $g_{PW}(r)$ at $r \approx 3$ Å corresponds to the second hydration layer and shows a more random distribution of water molecules, with some preference to waters pointing with hydrogens toward the peptide, particularly in the U state, Supporting Information Figure 3S.

Interestingly, the peptide−sorbitol pair correlation function $g_{PS}(r)$ shows a first peak at $r \approx 4$ Å, further than the first two hydration layers, representing sorbitol exclusion at these short distances from the peptide interface, Figure 2a. This exclusion is in agreement with other studies that have found that polyols are preferentially excluded from protein interfaces.[8,10,20] There are only minor differences in $g_{PW}(r)$ for the U and F states (see Supporting Information, Figure 4S), but for both states in the presence of sorbitol, the local densities of water in the first hydration layers relative to the bulk, seen as the height of the $g_{PW}(r)$ peaks, are somewhat higher than in pure water. This difference translates into ∼11 water molecules found in the vicinity of the peptide folded state ($r \leq 3.6$ Å) in the presence of sorbitol compared with ∼10 in pure water.

The net exclusion or accumulation of water or osmolytes near the solvated peptide (at infinite dilution) can be quantified either by the preferential hydration coefficient Γ or the preferential interaction coefficient for osmolyte Γ_S because these two are necessarily related.[8,16,36] We focus here on the preferential hydration Γ, which we have found in experiments to remain constant over a wide range of concentrations.[32,37] To find Γ in simulations, we use the operational definition[19,38]

$$\Gamma(R) = N_W\left(1 - \frac{N_S/N_W}{n_S/n_W}\right) \quad (1)$$

Here, we have defined a vicinal volume surrounding the peptide satisfying $r < R$, and a bulk domain for $r \geq R$ within the simulation box.[9] The values N_S and N_W represent the number of sorbitol and water molecules, respectively, within the vicinal volume, whereas n_S and n_W are the number of sorbitol and water molecules in the bulk domain. The preferential interaction coefficient Γ emerges as the converged value of $\Gamma(R)$ when R is large enough. A positive value for $\Gamma(R)$ represents preferential accumulation of water (or equivalently, exclusion of sorbitol) from the peptide interface, whereas a negative value indicates the depletion of water or accumulation of sorbitol.

Determining Γ from simulations is notoriously difficult.[39] Sufficient statistical sampling requires trajectories of 10 ns or longer, and convergence of values at a large enough R should be confirmed. Even then, preferential interaction coefficients are highly sensitive to the particular force fields used.[40] Indeed, we found that due to the overall sensitivity of $\Gamma(R)$, the profiles do not usually reach convergence for any single nanosecond segment along the MD trajectory. However, when we average over 15 ns out of the final 20 ns in the trajectory, values of $\Gamma(R)$ were well converged, as shown in Figure 2b. To ensure that only conformations representative of the U and F states are included in the averaging, the analysis of $\Gamma(R)$ was performed only on frames with a peptide ASA value that was lower than the mean value plus one standard deviation for the F state and higher than the mean value less one standard deviation for the U state. For the analyzed trajectory, $\Gamma(R)$ values for the U state converge at a large R to a positive value, $\Gamma_U \cong 9$, indicating preferential hydration, while for the F state Γ is slightly negative, $\Gamma_F \cong -5$, Figure 2b. Convergence of Γ values for the U state to a more positive value than for the F state indicates stronger sorbitol exclusion from U versus F conformations.

Thermodynamically, preferential interaction coefficients are directly related to the changes in peptide stability imposed by osmolytes. Our previous experiments[32] have shown that the peptide folding free energy ΔG_{UF} changes linearly with solute Osmolal concentration c_{Osm}, see inset in Figure 2b. Analogous changes in protein folding free energy due to cosolute addition are commonly described using the relation $\Delta G_{UF}(c_{Osm}) = \Delta G_{UF}(c_{Osm} = 0) + mc_{Osm}$, where the defined m value describes the constant slope in $\Delta G_{UF}(c_{Osm})$.[19,41] Importantly, this linearity in $\Delta G_{UF}(c_{Osm})$ translates into a constant change in the number of solute-excluding water molecules, $\Delta\Gamma_{UF}$, upon folding.[42] Thus, the Γ values evaluated in simulations for the different peptide states, F and U, can be used to calculate the change in peptide folding free energy upon the addition of solute, $\Delta\Delta G_{UF}(c_{Osm})$, as follows:

$$\Delta\Delta G_{UF}(c_{Osm}) = mc_{Osm} = \frac{RT}{55.6}(\Gamma_F - \Gamma_U)c_{Osm} = \frac{RT}{55.6}\Delta\Gamma_{UF}c_{Osm} \quad (2)$$

where 55.6 is the number of moles of water in 1 kg and RT is the thermal energy per mole. Experimentally, we have used the variation in $\Delta G_{UF}(c_{Osm})$ with sorbitol concentration, Figure 2b inset, to determine $\Delta\Gamma_{UF} = -19$. This indicates that, in the folding process, the preferential hydration of the peptide drops by 19, or alternatively, that 19 water molecules on average are "released" upon peptide folding, independent of sorbitol concentration.[32] This number corresponds closely with $\Delta\Gamma_{UF} = \Gamma_F - \Gamma_U = -14$ that we find in simulations, as described above. We note that our simulations use a somewhat higher concentration of sorbitol than in experiments, allowing us to observe larger changes in solution structure and to gain statistically significant and convergent results. Because experiments show a highly constant preferential hydration over a very large concentration regime, we expect the same trends to be valid also for the concentrations used in simulations.

An additional validation of the peptide simulations can be made by using the "transfer model" formalism.[13,36,43] It has been shown experimentally that changes in peptide free energy upon transfer from water to solutions containing cosolutes can be dissected into a sum of contributions from different amino acid side chains and backbone. These changes due to solvation can be translated into changes in folding free energy due to the presence of cosolutes, as long as values of accessible surface areas are available for both U and F states. Using the experimental values reported by Bolen and Auton,[36] we estimated the changes in solvation energies for the simulated folded and unfolded states. Specifically, using the exposed surface areas of side chains and the backbone in the different conformations of the U and F states of the peptide in water, we determine the average ensemble difference $\Delta\Delta G_{UF}(c_{Osm})$, see Figure 5S (Supporting Information). This procedure allowed us to derive the average m value using eq 2. Using the transfer model, we find $m = -646.14$ J mol^{-1}, which, is close to the experimental value of -841.36 J mol^{-1}.

Taken together, the correspondence of experimental and predicted m values, as well as the close match that we find in the experimental and simulated $\Delta\Gamma_{UF}$, further support our MD simulation as good models for the peptide in its solvating environment, allowing us to explore additional properties that are hardly accessible in experiments. Specifically, while $\Delta\Gamma_{UF}$ lets

us quantify the changes in preferential hydration upon folding in sorbitol solution, further analysis is required to reveal the underlying molecular origins for the exclusion. In the next sections, we proceed to the principal findings from our work to follow the possible molecular mechanism of peptide stabilization.

Hydrogen Bonding Plays a Major Role in Peptide Stabilization by Osmolyte. The experimentally determined enthalpic contribution to peptide folding in the presence of sorbitol[32] ($\Delta\Delta H_{UF} = -3.3$ kJ mol^{-1} for the folding in 1 Osm sorbitol solutions) could originate from a variety of forces acting in solution, such as altered van der Waals (vdW) interactions, electrostatic forces within media of an altered dielectric constant, and variations in hydrogen bonding. To begin to unravel the important contributions to the system enthalpy in simulations, we first calculated the total force-field energies, arising from Coulomb (U_{El}) and Lennard-Jones (U_{vdW}) contributions, Table 1. Examining the differences in the force field energies between the F and U states, we find a positive value for ΔU_{vdW} representing a Lennard-Jones contribution to the potential energy that disfavors folding, Table 1. In contrast to ΔU_{vdW}, ΔU_{El} shows a much larger, negative contribution and hence favors folding. The same trend is observed in the presence of sorbitol; however, the contributions of ΔU_{vdW}, as well as ΔU_{El} to the potential energy are smaller than in pure water. We conclude, therefore, that the dominating forces in the simulations leading to favorable folding are electrostatic. Importantly, hydrogen bonding is represented within the empirical force field primarily by electrostatic interactions, making it a potential source that drives folding.

Table 1. Differences between F and U States in Force Field Energies Arising from van der Waals or Coulomb Interactions, As Well As the PV Work Involved

	ΔU_{vdW}[a] (kJ/mol)	ΔU_{El}[b] (kJ/mol)	ΔU_{Tot}[c] (kJ/mol)	$P\Delta V$[d] (kJ/mol)
water	212.86	−1562.37	−1349.51	-1.56×10^{-3}
sorbitol 3.9 Osm	171.34	−765.35	−594.01	163.00×10^{-3}

[a] Total force-field energies arising from Lennard-Jones contributions. [b] Total force-field energies arising from Coulomb contributions. [c] Total force-field energies arising from Lennard-Jones and Coulomb contributions. [d] PV work calculated from the simulation for the transition from the U to the F state at a constant pressure of 1 atm and a volume corresponding to the same amount of water molecules around F and U states.

We also report in Table 1 values of ΔU_{Tot} representing the sum of ΔU_{vdW} and ΔU_{El} to the potential energy, as well as $P\Delta V$, where P is the pressure (1 atm in the simulation) and ΔV is the difference in the volume that includes the same amount of water molecules around F and U states. Under the simulation isobaric conditions, this $P\Delta V$ term represents the difference between the enthalpy and the energy of the system. We find that this difference is very small relative to ΔU_{Tot}, Table 1, and is also very small compared to the experimental value of $\Delta\Delta H_{UF}$. This allows us in the following discussion to equally speak about differences in the energy and the enthalpy.

To isolate the hydrogen bonding contribution to the changes in energy, we further analyzed changes to the hydrogen bonding network upon peptide folding in pure water and in the presence of sorbitol. Specifically, we enumerate the total number of hydrogen (H) bonds in the peptide solution and the number of internal peptide (PP) hydrogen bonds that are formed or lost upon folding. We use a geometric H bond definition, so that a hydrogen bond exists between two molecules if the oxygen−oxygen distance is less than $d = 3.5$ Å, and the O···O−H angle is smaller than $\theta = 30°$, as previously suggested.[44−46] This definition, as originally described for pure water, conveniently delineates contacts that form a prominent peak in the probability density of water−water nearest-neighbors as mapped in the d−θ plane. We have further verified that this definition is applicable to these contacts in the presence of polyols and sugars, as well as for water−sorbitol H bond interactions,[46] and that it also applies for the ternary system that includes the peptide, see the Supporting Information Figure 6S. The H bonds accounted for in the peptide environment include contributions from the different pairs of chemical species: water−water (WW), water−sorbitol (WS), water−peptide (WP), sorbitol−sorbitol (SS), and sorbitol−peptide (SP). For PP contacts, which also include nonhydroxyl types of H bonds, we use a slightly different definition described and evaluated by Thornton and McDonald.[47]

To evaluate changes in the number of H bonds in the different peptide states and solution conditions, we compared differences in numbers of bonds with respect to the average number of the same type of H bond in the bulk. By only counting the excess or deficit of bonds with respect to the bulk, n_{HB}, we are able to compare simulated systems that are slightly different in size or density. For this purpose, the bulk was defined as the volume satisfying $7.4 > r > 8.8$ Å from the peptide, where we find convergence in the difference in excess or deficit of bonds, for both the F and U states. Figure 3a indicates the difference

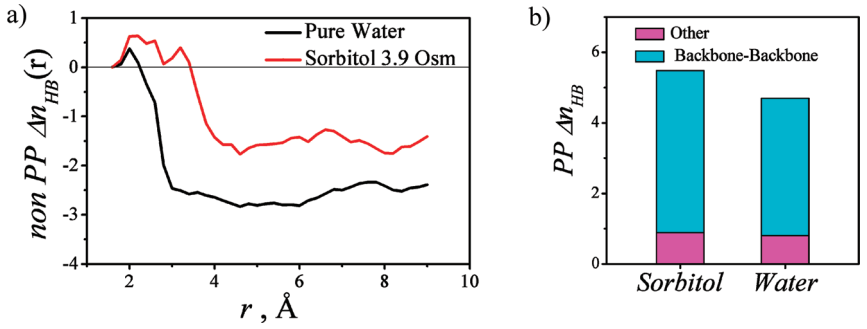

Figure 3. Difference in the number of hydrogen bonds in the folded and unfolded states in pure water and in the presence of sorbitol. (a) Hydrogen bonds in the peptide environment calculated with respect to the bulk versus the distance from any peptide atom. Hydrogen bonds in the peptide environment include water−water, water−sorbitol, water−peptide, sorbitol−sorbitol, and sorbitol−peptide hydrogen bonds. (b) Number of internal peptide hydrogen bonds.

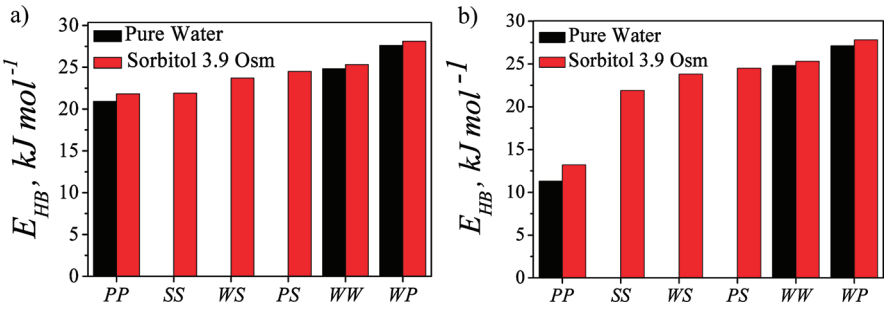

Figure 4. Average energies of each hydrogen bond in pure water and in the presence of sorbitol in the folded (a) and unfolded (b) states. All hydrogen bonds considered are within $r \leq 4$ Å, where r is the shortest distance from any peptide atom.

between F and U states in non-PP H bonds (non-PP $\Delta n_{HB}(r)$) in the peptide environment, plotted versus the distance r from any peptide atom. Negative values represent a loss of H bonds, while positive values represent gains in the number of hydrogen bonds upon folding.

Surprisingly, our analysis shows that by folding, the solvating environment loses hydrogen bonds in both pure water and in the presence of sorbitol. However, the loss is smaller in the presence of sorbitol, Figure 3a. Concomitantly, the number of internal peptide H bonds added in the U→F transition (PP Δn_{HB}) is also larger than in pure water, Figure 3b. We further dissected the number of internal peptide H bonds into backbone−backbone hydrogen bonds and all other PP H bonds. While the number of backbone−backbone H bonds is significantly larger in the presence of sorbitol, there is only a small difference in the corresponding numbers of nonbackbone−backbone H bonds. The trend for the changes in non-PP $\Delta n_{HB}(r)$ upon sorbitol addition is consistent with our experimental results that show a diminished unfavorable enthalpic contribution to folding in the presence of polyols.[32] This finding suggests an important contribution of H bonds in solution to the stabilizing effect of sorbitol.

To fully appreciate the effect of sorbitol requires that we not only follow the change in the numbers of H bonds but also account for variations in the strength of hydrogen bonds in the presence and absence of the osmolyte. Energies of each hydrogen bond (E_{HB}) were estimated using the correlation between H bond length and its strength, parametrized by Espinosa et al.,[48] and expressed as $E_{HB} = 2.5 \times 10^4 \exp(-3.6 \times d(H\cdots O))$, where d denotes the distance between the hydrogen atom and acceptor atom and E_{HB} is bond energy given in kilojoules per mole. We note that phenomenological energies derived using this parametrization are used here, as in other studies, only to provide a semiquantitative measure for the strength of H bonds.[49−51] Our analysis, therefore, relies only on the relative strength of the hydrogen bonds and not on their absolute values.

With the exception of PP hydrogen bonds, we find only small differences in H bond energies between the folded and unfolded states. Figure 4 shows the average energies for each class of H bond that are in close proximity to the peptide ($r \leq 4$ Å), both in pure water and in the presence of sorbitol. The small number of internal peptide H bonds that form in the U state, as well as the fact that these hydrogen bonds are relatively weak (compare 11.3 kJ/mol for U with 20.9 kJ/mol for F state in water) indicate an advantage to folding both in pure water and in the presence of sorbitol. In both states (U and F), we find that the WP contacts form the strongest H bonds (27.6 kJ/mol for F and 27.1 kJ/mol for U state in water). The relative strength of these H bonds grows in the presence of sorbitol (28.1 kJ/mol for F and 27.8 kJ/mol for U state in sorbitol). These WP H bonds are much stronger than PS hydrogen bonds (24.5 kJ/mol for both states). These rather weak PS bonds may, at least partly, explain sorbitol's exclusion from the peptide surface, and its preference to remain hydrated in the bulk solution, where the water−sorbitol hydrogen bond energy is ∼23.8 kJ/mol.

Interestingly, WW and PP hydrogen bonds are stronger in the presence of sorbitol than in pure water. This implies that water molecules released upon folding in the presence of sorbitol create hydrogen bonds with other water molecules in the bulk that are stronger than those that they form in pure water. In fact, every WW and WP hydrogen bond created in the presence of sorbitol gains an additional 0.5−0.8 kJ/mol over that formed in pure water.

Generally, hydrogen bond energies in simulations that use empirical force fields are not uniquely defined, as they arise in these models from electrostatic forces that originate from collective particle-charge interactions of many water molecules. We have, however, verified that another possible measure of hydrogen bond strength confirms our conclusions, as derived from the phenomenological estimates of Espinosa et al.[48] Specifically, we evaluated the force-field energy distribution for WW and WS contact pairs defined as H bonded, measured with respect to their energy at infinite separation. Using this alternate definition, we find that, in agreement with our conclusions from Figure 4, WW contacts are strengthened in the presence of sorbitol and that WW contacts are overall stronger than WS contacts, see Table 1S (Supporting Information).

To properly compound changes in H bond strength and changes in their numbers, we weigh the number of hydrogen bonds by the estimated energy of each hydrogen bond at each distance from the peptide. The resulting sum of hydrogen bond energies that includes all perturbations in H bonds around the peptide up to a distance r are compiled in Figure 5 for differences between the U and F states (ΔE_{HB}^{Tot}) in the presence and absence of sorbitol. We find that despite the loss in H bonds upon folding in the peptide environment, the peptide is overall enthalpically stabilized by changes in H bonding due to folding. In addition, we find larger peptide stabilization as a result of folding in the presence of the osmolyte, so that the H bond energy contributions converge to a value of ∼−72 kJ/mol in sorbitol versus ∼−48 kJ/mol in pure water.

While the choice of water and osmolyte model and force field may affect our results, particularly the hydrogen bond energies and solvation entropies, we do not expect other empirical force fields to yield qualitatively different results. Specifically, several studies using a variety of force fields for aqueous carbohydrate

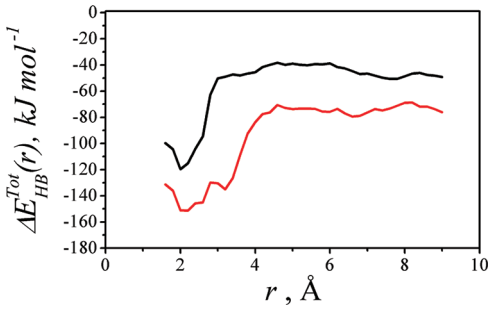

Figure 5. Cumulative hydrogen bond energy differences between the folded and unfolded states in pure water (black line) and in the presence of sorbitol (red line) calculated as the product of the number of hydrogen bonds and the estimated energy of each type of hydrogen bond. Summation is performed as a function of distance r from the peptide.

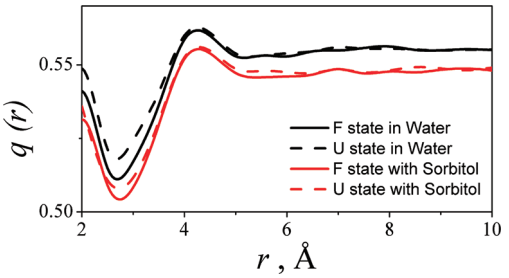

Figure 6. Tetrahedral structural order parameter, q, plotted as a function of distance r from the peptide. Order parameter $q(r)$ is shown in pure water (black) and in the presence of sorbitol (red) for folded (full lines) and unfolded (dashed lines) states.

binary solutions, including our own tests of additional force fields, have found similar effects of polyols on water structuring.[5] Moreover, another MD study of polyol interaction with large folded proteins that used a different force field (GROMOS96) has found several trends that are in common with our analysis, including a polyols-induced increase in the number of PP H bonds with a concomitant decrease in the number of PW bonds, increased protein hydration numbers, and stronger PW hydrogen bonds.[20]

Entropic Contributions and Water Orientational Order. An important and perhaps counterintuitive experimental result is that, in the presence of sorbitol, folding becomes *less* entropically favored ($\Delta\Delta S = -9$ J/mol K for folding at 1 Osm sorbitol).[32] To follow the possible sources of this decrease in the entropic contribution, we first studied the water tetrahedral structural order parameter $q(r)$, in pure water and in the presence of sorbitol, at distance r around folded and unfolded peptide conformations. This order parameter is a metric that has been used to quantify the tendency of a water molecule and its four nearest neighbors to adopt a tetrahedral arrangement[46,52] and is defined for the ith water molecule as

$$q_i = 1 - \frac{3}{8}\sum_{j>k}\left(\cos\psi_{ijk} + \frac{1}{3}\right)^2 \qquad (3)$$

where ψ_{ijk} is the angle formed between the central oxygen atom i and two neighboring atoms j and k (belonging to either water, polyol, or peptide hydroxyl oxygen or nitrogen), and the sum extends over four nearest neighbors. If oxygens (or nitrogens) are arranged in a perfect tetrahedral arrangement, then $q = 1$, while for an uncorrelated distribution of oxygens/nitrogens, $q = 0$.

We find a lower average value of q for sorbitol solutions relative to pure water, see Figure 6. We have also found a similar trend for the ordering of water around other polyol osmolytes in binary solutions in the absence of a peptide.[46] The decrease in $q(r)$ values for $r < 4$ Å indicates that the peptide further imposes a destructuring effect on hydrating waters found in its close proximity. A similar conclusion was reported previously by Czapiewski and Zielkiewicz, who investigated the structural and dynamic properties of water in the solvation shell formed around different conformations of a polypeptide chain in pure water.[53] By following the two-particle entropy around the peptide core, they concluded that water around the peptide is (locally) less structured than in the bulk.

The order parameter further indicates that water is less tetrahedrally structured around F than U conformations, Figure 6. Moreover, the difference between q values in the peptide's vicinity for F and U states in pure water is larger than in the presence of sorbitol. These findings suggest that the presence of sorbitol imposes a disordering effect on water, so that both the peptide F and U states no longer alter water structuring to the same extent as in pure water.

To further investigate the structural properties of water within the first solvation layers, we determine the water angular probability distribution in term of cos θ and ϕ, corresponding to the two angles that describe the orientation of water molecules with respect to the peptide within 4 Å from any peptide atom, as described in the Methods. Figure 7 shows the *difference* in the water angular probability distribution between folded and unfolded states, in pure water and in the presence of sorbitol.

The difference in water's angular distribution is very close to zero in the presence of sorbitol, indicating a similar distribution of water molecules' orientations in close vicinity to F and U states. However, in pure water, we find a considerably larger difference, for example, in the population of water orientations with $-0.6 < \cos\theta < -0.9$ and $45 < |\phi| < 90$. Semiquantitatively, this larger probability difference in water orientations translates to a larger orientational entropy decrease for folding in pure water through the known expression for information entropy,[54] $S = -k_B \Sigma_i P_i \ln P_i$ that relates the probability of accessible states i to the entropy S. These results also correlate well with the difference in q values around F and U states, as discussed above.

There are, in fact, many potential sources of entropy in this three-component system. As we have shown, an important entropic contribution relates to the changes in water orientation due to the addition of a peptide to solution. Therefore, to accurately evaluate the part of the solvation entropy that is due to the orientational degree of freedom of water molecules with respect to the peptide (s^2_{PW}), we calculate $s^2_{PW,o}$ and $s^2_{PW,r}$ that describe the orientational and radial parts of the solvation entropy, respectively (see Methods for details). Summarized in Table 2, we show $s^2_{PW,o}$ and $s^2_{PW,r}$ calculated for the F and U states and compare the differences between folded and unfolded states, $\Delta s^2_{PW,o}$ and $\Delta s^2_{PW,r}$, to the experimentally determined entropy of folding.

In water, the values of the orientational entropy $s^2_{PW,o}$ for the folded (-807.50 J/mol K) and unfolded (-1152.87 J/mol K) states are much lower than in the presence of sorbitol (-89.06 J/mol K and -131.99 J/mol K for F and U states, respectively). The larger orientational freedom in water may be explained by our previous findings, indicating that, even in the absence of

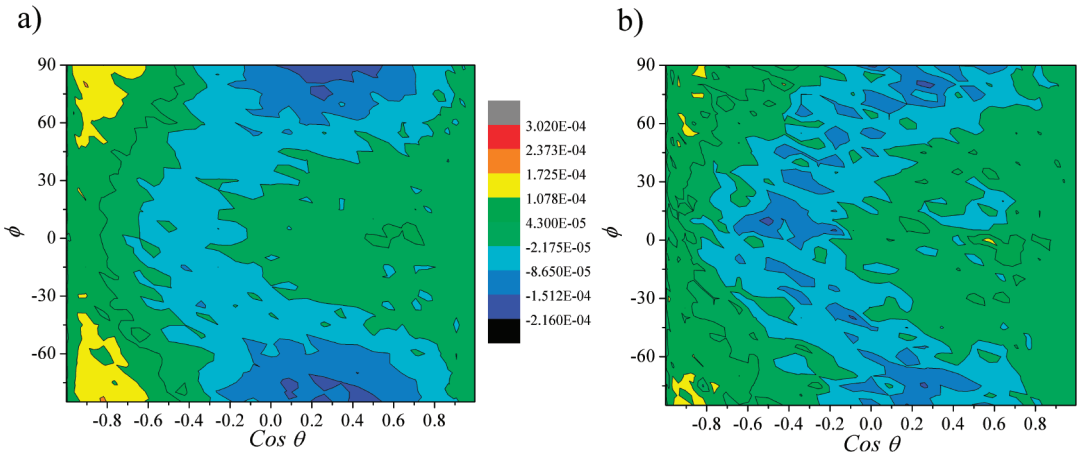

Figure 7. Difference in water angular probability distribution between folded and unfolded states in pure water (a) and in the presence of sorbitol (b).

Table 2. Different Contributions to the Solvation Entropy[a]

		$s^2_{PW,o}$	$s^2_{PW,r}$	$\Delta s^2_{PW,o}$	$\Delta s^2_{PW,r}$	ΔS_{exp}
pure water	folded	−807.50	−3.78	345.37	0.45	44
	unfolded	−1152.87	−4.23			
sorbitol 3.9 Osm	folded	−89.06	1.49	42.93	2.07	35
	unfolded	−131.99	−0.58			

[a] All contributions are given in units of J/mol K. $s^2_{PW,o}$ denotes the orientational parts and $s^2_{PW,r}$, the radial parts.

peptide, the binary sorbitol solution is more disordered than pure water.[46] Thus, the addition of the peptide to the binary solution cannot further increase water's orientational disorder to the same extent as it does in pure water.

It has been established that the solvation entropy s^2_{PW} is typically strongly dominated by the orientational part.[55] Accordingly, we find that the orientational entropy gain for folding in water ($\Delta s^2_{PW,o}$ = 345.37 J/mol K) is larger than in the presence of sorbitol ($\Delta s^2_{PW,o}$ = 42.93 J/mol K), while changes in the radial part are significantly smaller, Table 2. This result is also in good qualitative agreement with our experimental results that show diminished favorable entropy for folding once osmolytes (including sorbitol) are added.[32] These findings point to water orientational degree of freedom as an important contribution that should be considered, together with additional possible entropic contributions to the folding free energy of the peptide.

DISCUSSION

Recently, the mechanism by which polyols and sugar osmolytes impact peptide stability has been shown to be enthalpically driven.[32] The current study aims to resolve the molecular origins of this enthalpic mechanism, by simulating the folded (β-hairpin, F state) and unfolded (U) states of a model peptide in pure water and in the presence of sorbitol.[33,56,57] Sorbitol was shown experimentally to significantly shift the thermodynamic equilibrium of the peptide, making it a convenient model for stabilizing polyol osmolytes.

Using molecular dynamics simulations, we find that solution structure is modified upon peptide addition, but these changes are somewhat different in the presence and absence of sorbitol. In the following sections, we describe these differences and show how these modulations can explain the additional enthalpic peptide stabilization found in the presence of sorbitol.

Sorbitol Alters the Peptide Hydration Layer. Whereas recent works have argued that the presence of osmolytes alters protein stability indirectly by affecting water structure,[5−7,20] a case has also been made that it is the direct interaction between osmolyte and protein, or steric (excluded volume) interactions, that mediate the osmolyte effect.[9,12,58,59] The interplay of direct interactions and hydration has been particularly important in explaining the action of various solutes such as urea[51,60] or TMAO.[61] Our simulations indicate that while polyols remain excluded from the first solvation layer around peptide, they drive peptide stabilization primarily by impacting that first hydration layer. Specifically, local changes in concentrations and in hydrogen bonding relative to the bulk upon sorbitol addition are all shown to be limited to the peptide's first hydration layers, see Figures 2, 3a, 5, and 6.

The higher values of peptide−water $g(r)$ hydration peaks in the presence of sorbitol compared with their value in pure water suggest a larger accumulation of water molecules around the peptide when sorbitol is present, see Figure 2. It may be tempting to speculate that this accumulation will result in an increase in the number of available hydrogen bonds for peptide−water interactions in the presence of sorbitol; however, in simulations we find an opposite trend, as further discussed in the following.

The overall change in the number of sorbitol-excluding water molecules (preferential hydration) upon peptide folding from the U to F states in our simulations is close to the values derived experimentally ($\Delta\Gamma_{UF} \approx -14$ and -19 in simulation and experiments, respectively).[32] This release of sorbitol-excluding waters should inevitably incur an enthalpic contribution, analogous to the heat of dilution associated with adding pure water to a binary aqueous sorbitol solution, ΔH_m^{dil}.[62−64] Interestingly, ΔH_m^{dil} for the corresponding number of waters released into 1 m sorbitol solution is ∼−0.225 kJ/mol.[64] This value can account for only ∼10% of the peptide folding enthalpy change found experimentally in the presence of sorbitol. This result highlights the stark difference between the released osmolyte-excluding waters and pure bulk water. Specifically, the peptide interfacial waters can be expected to be much different than bulk waters, both structurally and in their interactions with peptide and solution.

Solution−Peptide and Internal Peptide Hydrogen Bonds Drive Peptide Stabilization. It is instructive to dissect the converged cumulative hydrogen bond energies, shown in Figure 5, into solution−peptide H bonds (including WP and SP), solution H bonds (including WW, WS, and SS), and internal

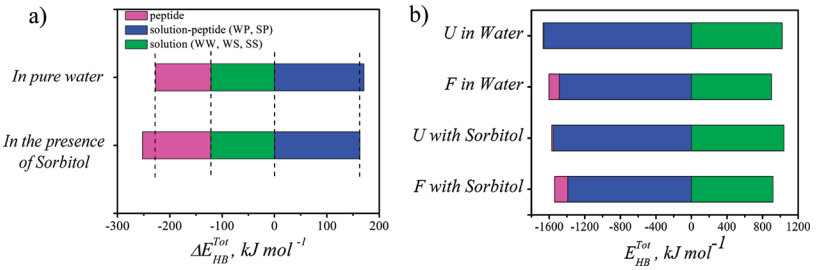

Figure 8. Cumulative hydrogen bond energies dissected into internal peptide, solution−peptide, and solution hydrogen bonds. (a) Differences between F and U states in pure water and in 3.9 Osm sorbitol. (b) F and U states in pure water and in the presence of sorbitol. Solution−peptide hydrogen bonds include WP and SP hydrogen bonds. Solution hydrogen bonds include WW, WS, and SS hydrogen bonds.

peptide H bonds. Figure 8a shows the energy differences between folded and unfolded states ΔE_{HB}^{Tot} in each of these categories. Solution H bond energy differences are almost the same in pure water and aqueous sorbitol solution. However, the energies of solution−peptide and internal peptide hydrogen bonds significantly change in the presence of sorbitol. These changes are manifested in reduced solution−peptide hydrogen bond energy losses, as well as an increased internal peptide hydrogen bond energy gain upon folding in the presence of sorbitol, Figure 8.

Changes in Cumulative Hydrogen Bond Energies Track the Changes in Number of Hydrogen Bonds. Figure 8b shows the dissected cumulative hydrogen bond energies for the U and F peptide states in pure water and in the presence of sorbitol. While we found an increase in the energy of all H bond types in the presence of sorbitol (Figure 4), we concurrently found lower total solution−peptide H bond energies in the presence of sorbitol for both F and U states, Figure 8b. This finding reflects the smaller overall number of solution−peptide hydrogen bonds that form in the presence of sorbitol. This smaller number of bonds is also responsible for the decrease in the number of hydrogen bonds lost upon folding in sorbitol, see Figure 3a. Some of these H bonds lost are peptide−water hydrogen bonds that are the strongest H bonds formed in this system. To compensate for the loss of these H bonds as a result of folding, the system tends to increase the number of internal peptide hydrogen bonds, significantly strengthens these (seen as shorter bond length d), and in addition creates stronger hydrogen bonds between peptide and water (27.8 and 28.1 kJ/mol for U and F states, respectively). We further find that the increase in internal peptide hydrogen bond enthalpy upon folding in the presence of sorbitol, Figure 8a,b, is mostly due to the higher number of backbone−backbone H bonds, see Figure 3b. This finding is also consistent with the work of Bolen and co-workers,[4] who have recently shown an enhancement of protein backbone−backbone hydrogen bonding interactions upon dilution from a good solvent (urea solution) to poorer (osmolytes containing) solvents, such as sarcosine or TMAO aqueous solutions.

Reduced Numbers of Available Hydrogen Bonds in the Presence of Sorbitol Arise from Polyol's Ability to Form H Bonds. Polyols are known to compete with water's own tendency to create optimal hydrogen bonds, thereby leading to a smaller number of solution−peptide hydrogen bonds that can form in their presence.[46,53] The smaller number of potential hydrogen bonds in the peptide vicinity in the presence of sorbitol also results in a smaller number of these bonds that can be lost as a result of folding. Overall, we have previously shown that polyols tend to participate in forming weaker, more distorted hydrogen bonds, in this way disrupting the water hydrogen bonding network and allowing less tetrahedral arrangements.[20,32,52] In concert, water molecules tend to optimize remaining water−water H bonds by creating more linear and shorter contacts leading to stronger interactions.[20,46] Indeed, we find here that sorbitol strengthens water−water as well as water−peptide hydrogen bonds, Figure 4. This impact of osmolytes on solution structure is somewhat similar to that shown in previous simulation studies of another known protective osmolyte, TMAO, showing a modest enhancement of the water structure near TMAO as well as an increase in water−water hydrogen bonding.[7]

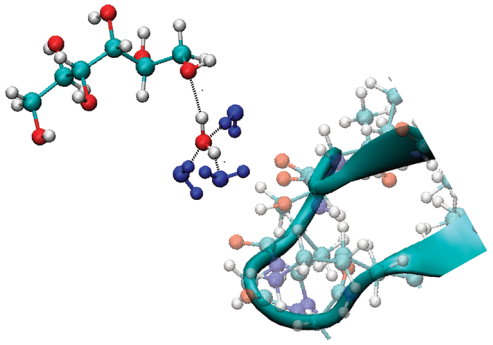

Figure 9. Typical snapshot from MD simulation of peptide in sorbitol solution, showing a water molecule that forms a weak H bond contact with sorbitol but three strong, optimized H bonds with waters around it.

The emerging picture of solution structure can be summarized in a typical simulation snapshot, Figure 9. The image shows a water molecule in the peptide's first hydration layer that forms a weak hydrogen bond contact with sorbitol that is located further from the peptide but makes three much stronger hydrogen bonds with water molecules within that solvation layer. These H bonds with neighboring waters are even closer to optimal than water in the bulk, see Figure 7S. We find that this type of configuration is statistically favored and that sorbitol tends to reduce the number of hydrogen bonds with which the peptide can potentially interact. Sorbitol addition may, therefore, be viewed as introducing a competition between peptide and osmolyte for hydrogen bonding with water. Due to this competition, some potential H bonds to the peptide are lost, forcing the peptide to optimize remaining H bonds with water or within itself. This view also explains how water accumulation in the peptide solvation shell, discussed in Results, coincides with fewer yet stronger H bonds between water and peptide in the presence of sorbitol. Interestingly, Collins and Washbaugh[65] suggested an analogous mechanism for the alteration of water structuring at interfaces due to solutes to describe the action of different salt solutes.

Our results indicate that peptide-sorbitol H bonds are weaker and less favorable than other H bonds that can form in the ternary mixtures. This weaker interaction leads to sorbitol's exclusion and to preferential hydration of the peptide. In terms of polymer theory, polyol solutions are poorer solvents to the peptide than water, and therefore promote its collapse.[66,67] This forces the peptide to optimize internal (primarily backbone−backbone) hydrogen bonds. These findings gain support from the experimental studies of Bolen and coauthors,[4,12,68] showing that the unfavorable interactions between osmolytes and the peptide backbone raise the free energy of the U state, thereby shifting the thermodynamic equilibrium toward the native state. Non-hydrogen bonded "hydrophobic" interactions between nonpolar parts of the peptide are important for the collapse, but seem to be less altered by the presence of sorbitol than the hydrogen bonding network.

Hydrogen Bond Optimization Is Consistent with a Decrease in Peptide Solvation Entropy in the Presence of Sorbitol. To follow the contribution of water structural properties within the peptide hydration shell to the solvation entropy, we used the two-particle approximation to configurational entropy. We focused here on two terms of the water solvation entropy, the orientational and radial entropy contributions, and followed changes in peptide solvation entropy as a result of folding in sorbitol solution. This analysis revealed restriction in water orientations in the presence of sorbitol and a dominant contribution of orientational entropy ($\Delta\Delta s^2_{PW,o} = -302.44$ J/mol K compared with $\Delta\Delta s^2_{PW,r} = 1.62$ J/mol K). The decrease in solvation entropy results from the optimization of hydrogen bonds wrought by the presence of sorbitol that concomitantly restricts the orientational freedom of water. This entropic contribution agrees with the trends found experimentally, showing a decrease in the total favorable entropic contribution to folding as a result of sorbitol addition ($\Delta\Delta S = -9$ J/mol K for folding at 1 Osm sorbitol).[32]

Other terms in the total entropy that are more hardly accessible computationally could be important, but previous studies have shown that their contribution is typically limited. For example, estimates of the term depending on water−water interactions, s^2_{WW}, were calculated by Zielkiewicz and Czapiewski for water within a peptide solvation layer;[53] the study concluded that the local structure of the solvating water changes only slightly compared to that of bulk water. We suggest, therefore, that this term is expected to have a smaller influence also on the solvation entropy in the presence of sorbitol.

The Possible Contribution of Crowding. In addition to these entropic contributions, there are other sorbitol-related entropic terms that have not been explicitly determined here. For example, a calculation of depletion entropy can be made on the basis of the number of water molecules released as a result of peptide folding in sorbitol solution[32] according to Asakura−Oosawa theory.[69] A simple estimate results in $\Delta\Delta S_{dep} = \Pi\Delta V = \Pi\Delta\Gamma_{UF}\nu N_{Av} \approx 10$ J/mol K for a solution osmotic pressure of $\Pi = 3.9$ Osm at $T = 298$ K, where ΔV is the change in the osmolyte's free volume due to folding, as determined in ref 32, and ν is the volume of a water molecule. This value can account only for a small part of the total change in entropy and would suggest that the folded state is entropically more favored in the presence of sorbitol, contrary to what we found experimentally. This suggests that mechanisms that rely purely on steric interactions do not play the dominant role in sorbitol's action.

Experiments further showed that the enthalpically driven mechanism together with the entropic penalty associated with the native state stabilization are strongly osmolyte size-dependent.[32] Thus, the entropic penalty grows as cosolute is varied from smaller polyols to the larger carbohydrates in the order glycerol < sorbitol < trehalose. This, again, is in contrast to a pure volume exclusion mechanism that would dictate a stronger but more favorable entropic contribution to folding when larger molecular crowders are present at the same mole concentration. These findings are, however, in agreement with recent experiments on the stabilization (or destabilization) of DNA in the presence of polyethylene glycols of various molecular weights.[70] These experiments showed a size-dependent exclusion that could be dissected into the extent of monomer−macromolecule "chemical interaction" effect and a steric effect. Interestingly, the steric effect becomes stronger with the volume of the crowder molecule, while the chemical interaction contribution is proportional to macromolecule and cosolute interacting surface areas. In agreement, we find that for the polyols we have tested,[32] the entropic penalty grows with cosolute size but that the slope of this change becomes less steep as cosolute size becomes larger, possibly suggesting a larger entropically favorable steric contribution for the larger cosolutes.

CONCLUSION

We have used MD simulations to analyze the mechanism of peptide stabilization by sorbitol. Contrary to common wisdom, the peptide stabilization imposed by polyols was found experimentally to be enthalpically and not entropically driven. The emerging molecular mechanism shows that sorbitol stabilizes the native folded state of peptides by changing their immediate solvation layer. These changes lead to a decrease in the number of hydrogen bonds lost as a result of folding, optimization of existing hydrogen bonds, and an increase in the number of internal peptide hydrogen bonds. While the effects of sorbitol described in this study for a short 16-amino-acid-long peptide are relatively small, the significant accumulation of small contributions from solute−peptide interactions over extended macromolecular interfaces should have a profound effect on stabilization of the larger proteins typically found in cellular environments. It will be interesting to find out if the described mechanism is common to all peptides with different sequences and secondary structures, as well as to proteins, in solutions that contain polyols or other osmolytes.

METHODS

All-Atom Molecular Dynamics Simulations. To compare with our previous experimental work,[32] we simulate here a model 16-residue peptide (sequence: Ac-KKYTVSINGKKITVSI) that can fold to a β-hairpin structure. Unfolded and folded peptide states were simulated in pure water and in the presence of sorbitol. To select initial configurations for subsequent MD simulations, we first employed the CHARMM empirical force field with implicitly included water to distinguish between the two primary states: folded and unfolded. An all-atom representation of the peptide was used in these simulations together with the SASA implicit water parameters, at two temperatures: 300 K and 400 K. Statistics of peptide dynamics showed two major peptide conformational populations when dissected by their accessible surface area (ASA), see Supporting Information Figure 1S. These results indicate conformations and changes in peptide folding that are similar to those found using NMR measurements,[33] indicating

Table 3. Parameters for Simulation Runs

peptide state	sorbitol (Osm)	number of sorbitol molecules	number of water molecules
folded (F)	0	0	3769
	3.9	150	2174
unfolded (U)	0	0	3747
	3.9	150	2169

that for different effective temperatures, the peptide occupies a different set of accessible conformations, changing from a more compact and folded β-hairpin structure at low temperatures to more extended "unfolded" structures with a larger ASA at high temperatures. One of the most probable structures from each state was used for further all-atom MD simulations with explicit water performed using NAMD.[71]

Table 3 lists the entire set of the MD simulations performed. Conformations of the folded and unfolded states were placed in a cubic box of TIP3P water molecules and three chloride counterions (representing pure water solvent solutions). In addition, each state was also immersed in osmolyte solutions by inserting sorbitol molecules in a cubic box of TIP3P water molecules with a single peptide molecule, corresponding to concentrations of approximately 3.9 Osm (3.86 *m*), as detailed in Table 3. All interactions were subject to the CHARMM27 force field[72,73] and used without further modifications. Bonds were kept at a constant length for solutes and solvent molecules using the SHAKE algorithm. All simulations were performed within the NPT ensemble, at $T = 298$ K (using Langevin dynamics algorithm as implemented in NAMD) and $P = 1$ bar (maintained using the Nose−Hoover Langevin piston method), within a cubic box with fluctuating length of ca. $L = 48$ Å and periodic boundary conditions. After initial energy minimization of 1000 steps and 100 ps of MD equilibration, 50 ns MD simulation trajectories were collected. Of these, the last 13−15 ns were used for further analysis, with collection steps every 0.5 ps, resulting in well converged averages for all calculated distributions. The time step in all simulations was 2 fs. Electrostatic calculations were performed using the Ewald particle-mesh summation with 1 Å grid spacing. The van der Waals interactions were truncated smoothly with a cutoff of 12 Å and a switching distance of 10 Å. MD trajectory analysis was performed using VMD.[74]

Radial Distribution Functions. Radial distribution functions, $g_{xy}(r)$, assess local densities of atom type y at a distance r from an atom of type x. This $g_{xy}(r)$ is calculated as

$$g_{xy}(r) = \frac{y(r',r)}{\rho_{y,\mathrm{bulk}}\delta V(r',r)} \tag{4}$$

where r is the radius of the solvation shell, $y(r',r)$ is the number of y molecules found between r' and r, $\delta V(r',r)$ is the volume of the shell ranging from r' to r, and $\rho_{y,\mathrm{bulk}}$ is the bulk density of y. The volume $\delta V(r',r)$ was calculated using the Monte Carlo method for determining volume by randomly placing 1000 points in the simulation box and computing the ratio of hits within a shell to the total number of points. Unless otherwise stated, in all of our reported calculations, we have evaluated local densities of water oxygen's and sorbitol's center of mass at a distance r, corresponding to the shortest distance from *any atom* of folded or unfolded peptide states.

Osmolyte Force-Field Validation. We have previously validated the sorbitol parameter set used here[46] by comparing densities from binary mixture simulations of sorbitol at 2.4 M to the densities extrapolated from experimental data[75] (1.14 gr/cm^3). The experimental value differs by 3% from the value found in our simulations (1.11 gr/cm^3). In addition, we have calculated another experimentally available thermodynamic property, the Kirwood−Buff integral for sorbitol[46] $G_{SS} = \int (g_{ss} - 1)\, d\nu$, where S stands for solute, and g_{SS} is the solute−solute pair correlation function, measured as a function of the distance between a central polyol hydroxyl oxygen and an osmolyte-representing atom. We found that in simulations $G_{SS} = -0.2$, very close to the previously published experimental value of -0.23.[76]

Calculation of the Two-Body Peptide−Water Contribution to the Solvation Entropy. The position and orientation of each water molecule with respect to the peptide were determined from the MD trajectories and used within the two-particle approximation to find the contribution of the local structure of water to the solvation entropy, as has been previously developed and described in detail (see refs 53, 55, 77). Within this approximation, the two-particle contribution to entropy evaluated relative to a completely random orientation of water molecules for a two-component system has the form:[55,77,78]

$$s^2 = s^2_{PP} + s^2_{PW} + s^2_{WW} \tag{5}$$

where s^2_{PP} describes peptide−peptide interactions and therefore is irrelevant in our one-peptide simulations. The $s_{WW}{}^2$ term is harder to access and is expected to be less important for the differences between solutions with and without peptides, as further detailed in the Discussion. Finally, $s_{PW}{}^2$ describes the protein−water interactions given by

$$s^2_{PW} = -k_B N_W \rho \int g^2_{PW} \ln g^2_{PW}\, d\bar{r} + kN_W \rho \int (g^2_{PW} - 1)\, d\bar{r} \tag{6}$$

where ρ denotes the number density of the peptide, taking into account the volume within 4 Å from each peptide atom, $g_{PW}{}^2$ is the two-body peptide−water distribution function, N_W is the number of water molecules within the same volume, and k_B is Boltzmann's constant.

The two-body contribution to the solvation entropy can be further separated into an orientational $s^2_{PW,o}$ and a radial (or "non-orientational") $s^2_{PW,r}$ part by writing g^2_{PW} as a product, $g^2_{PW} = g(r)\, a(r,\theta,\phi)$, of the radial distribution function $g(r)$ and a function $a(r,\theta,\phi)$ that describes the orientation of water molecules (the angular distribution function), normalized to 4π. The angles θ and ϕ determine the position of the surrounding water molecules relative to the closest peptide atom.[78] The angle θ describes the angle between the dipole moment of the water molecule, d, and the vector originating at the water molecule's oxygen atom and ending at the closest peptide atom, r_{OP}. The angle ϕ is formed between the plane spanned by the water molecule and the plane spanned by the d and r_{OP} vectors.[78] Using the product that gives g^2_{PW} in the expression for s^2_{PW}, we thus obtain $s^2_{PW} = s^2_{PW,o} + s^2_{PW,r}$,

where

$$s^2_{PW,r} = -4\pi k N_W \rho \int_0^\infty [g(r)\ln g(r) - g(r) + 1] r^2\, dr \quad (7)$$

$$s^2_{PW,o} = -kN_W\rho \int_0^\infty r^2\, g(r)\, dr \times \int_0^\pi \int_0^{2\pi} a(r,\theta,\phi)\ln a(r,\theta,\phi)\sin\theta\, d\theta\, d\phi \quad (8)$$

In our evaluations of these quantities, we used the following integration steps: $\delta r = 0.2$ Å and $\delta\theta = \delta\phi = \pi/36$.

■ ASSOCIATED CONTENT

Supporting Information. Figures for the probability distribution of accessible surface area of the peptide under different conditions, the average number of water molecules around the different peptide amino acids, radial distribution functions for water oxygens in the peptide vicinity, properties of hydrogen bonds and their probability distributions, and the average energy of hydrogen bonds in the bulk. This material is available free of charge via the Internet at http://pubs.acs.org.

■ AUTHOR INFORMATION

Corresponding Author

*Tel.: 972-2-6585484. Fax: 972-2-6513742. E-mail: daniel@fh.huji.ac.il.

■ ACKNOWLEDGMENT

We thank Hirsh Nanda for his help with setting up the implicit solvent simulations and Liel Sapir for his help with the transfer free energy calculations. The financial support from the Israel science foundation (ISF grant Nos. 1011/07 and 1012/07) is gratefully acknowledged. The Fritz Haber Research Center is supported by the Minerva Foundation, Munich, Germany.

■ REFERENCES

(1) Yancey, P. H.; Clark, M. E.; Hand, S. C.; Bowlus, R. D.; Somero, G. N. Living with Water-Stress - Evolution of Osmolyte Systems. *Science* **1982**, *217* (4566), 1214–1222.

(2) Willmer, P. Biochemical adaptation - Mechanism and process in physiological evolution. *Science* **2002**, *296* (5567), 473–473.

(3) Wood, J. M. Osmosensing by bacteria: Signals and membrane-based sensors. *Microbiol. Mol. Biol. Rev.* **1999**, *63* (1), 230.

(4) Holthauzen, L. M. F.; Rosgen, J.; Bolen, D. W. Hydrogen Bonding Progressively Strengthens upon Transfer of the Protein Urea-Denatured State to Water and Protecting Osmolytes. *Biochemistry* **2010**, *49* (6), 1310–1318.

(5) Sharp, K. A.; Madan, B.; Manas, E.; Vanderkooi, J. M. Water structure changes induced by hydrophobic and polar solutes revealed by simulations and infrared spectroscopy. *J. Chem. Phys.* **2001**, *114* (4), 1791–1796.

(6) Freda, M.; Onori, G.; Santucci, A. Hydrophobic hydration and hydrophobic interaction in aqueous solutions of tert-butyl alcohol and trimethylamine-N-oxide: a correlation with the effect of these two solutes on the micellization process. *Phys. Chem. Chem. Phys.* **2002**, *4* (20), 4979–4984.

(7) Zou, Q.; Bennion, B. J.; Daggett, V.; Murphy, K. P. The molecular mechanism of stabilization of proteins by TMAO and its ability to counteract the effects of urea. *J. Am. Chem. Soc.* **2002**, *124* (7), 1192–1202.

(8) Rosgen, J.; Pettitt, B. M.; Bolen, D. W. An analysis of the molecular origin of osmolyte-dependent protein stability. *Protein Sci.* **2007**, *16* (4), 733–743.

(9) Athawale, M. V.; Dordick, J. S.; Garde, S. Osmolyte trimethylamine-N-oxide does not affect the strength of hydrophobic interactions: Origin of osmolyte compatibility. *Biophys. J.* **2005**, *89* (2), 858–866.

(10) Rosgen, J.; Pettitt, B. M.; Bolen, D. W. Protein folding, stability, and solvation structure in osmolyte solutions. *Biophys. J.* **2005**, *89* (5), 2988–2997.

(11) Auton, M.; Bolen, D. W. Application of the transfer model to understand how naturally occuring osmolytes affect protein stability. *Osmosensing Osmosignaling* **2007**, *428*, 397−418.

(12) Bolen, D. W.; Baskakov, I. V. The osmophobic effect: Natural selection of a thermodynamic force in protein folding. *J. Mol. Biol.* **2001**, *310* (5), 955–963.

(13) O'Brien, E. P.; Ziv, G.; Haran, G.; Brooks, B. R.; Thirumalai, D. Effects of denaturants and osmolytes on proteins are accurately predicted by the molecular transfer model. *Proc. Natl. Acad. Sci. U. S. A.* **2008**, *105* (36), 13403–13408.

(14) Kornblatt, J. A.; Kornblatt, M. J. The effects of osmotic and hydrostatic pressures on macromolecular systems. *Biochim. Biophys. Acta—Protein Struct. Mol. Enzymol.* **2002**, *1595* (1−2), 30–47.

(15) Cayley, S.; Record, M. T. Roles of cytoplasmic osmolytes, water, and crowding in the response of Escherichia coli to osmotic stress: Biophysical basis of osmoprotection by glycine betaine. *Biochemistry* **2003**, *42* (43), 12596–12609.

(16) Timasheff, S. N. In disperse solution, "osmotic stress" is a restricted case of preferential interactions. *Proc. Natl. Acad. Sci. U. S. A.* **1998**, *95* (13), 7363–7367.

(17) Bolen, D. W. Effects of naturally occurring osmolytes on protein stability and solubility: issues important in protein crystallization. *Methods* **2004**, *34* (3), 312–322.

(18) Gibbs, J. W. On the equilibrium of heterogeneous substances. *Trans. Connecticut Acad.* **1876/78**, *3* (108−248), 343–542.

(19) Parsegian, V. A. Protein-water interactions. *Int. Rev. Cytol. Survey Cell Biol.* **2002**, *215*, 1−31.

(20) Liu, F. F.; Ji, L.; Zhang, L.; Dong, X. Y.; Sun, Y. Molecular basis for polyol-induced protein stability revealed by molecular dynamics simulations. *J. Chem. Phys.* **2010**, *132*, 22.

(21) Parsegian, V. A.; Rand, R. P.; Rau, D. C. Osmotic stress, crowding, preferential hydration, and binding: A comparison of perspectives. *Proc. Natl. Acad. Sci. U. S. A.* **2000**, *97* (8), 3987–3992.

(22) Linhananta, A.; Hadizadeh, S.; Plotkin, S. S. An Effective Solvent Theory Connecting the Underlying Mechanisms of Osmolytes and Denaturants for Protein Stability. *Biophys. J.* **2011**, *100* (2), 459–468.

(23) Saunders, A. J.; Davis-Searles, P. R.; Allen, D. L.; Pielak, G. J.; Erie, D. A. Osmolyte-induced changes in protein conformation equilibria. *Biopolymers* **2000**, *53* (4), 293–307.

(24) Patel, C. N.; Noble, S. M.; Weatherly, G. T.; Tripathy, A.; Winzor, D. J.; Pielak, G. J. Effects of molecular crowding by saccharides on alpha-chymotrypsin dimerization. *Protein Sci.* **2002**, *11* (5), 997–1003.

(25) O'Connor, T. F.; Debenedetti, P. G.; Carbeck, J. D. Simultaneous determination of structural and thermodynamic effects of carbohydrate solutes on the thermal stability of ribonuclease A. *J. Am. Chem. Soc.* **2004**, *126* (38), 11794–11795.

(26) Pincus, D. L.; Hyeon, C.; Thirumalai, D. Effects of trimethylamine N-oxide (TMAO) and crowding agents on the stability of RNA hairpins. *J. Am. Chem. Soc.* **2008**, *130* (23), 7364–7372.

(27) McPhie, P.; Ni, Y. S.; Minton, A. P. Macromolecular crowding stabilizes the molten globule form of apomyoglobin with respect to bath cold and heat unfolding. *J. Mol. Biol.* **2006**, *361* (1), 7–10.

(28) Cheung, M. S.; Klimov, D.; Thirumalai, D. Molecular crowding enhances native state stability and refolding rates of globular proteins. *Proc. Natl. Acad. Sci. U. S. A.* **2005**, *102* (13), 4753–4758.

(29) Zhou, H. X.; Rivas, G. N.; Minton, A. P. Macromolecular crowding and confinement: Biochemical, biophysical, and potential physiological consequences. *Ann. Rev. Biophys.* **2008**, *37*, 375–397.

(30) Stanley, C. B.; Strey, H. H Osmotically induced helix-coil transition in poly(glutamic acid). *Biophys. J.* **2008**, *94* (11), 4427–4434.
(31) Jiao, M.; Li, H. T.; Chen, J.; Minton, A. P.; Liang, Y. Attractive Protein-Polymer Interactions Markedly Alter the Effect of Macromolecular Crowding on Protein Association Equilibria. *Biophys. J.* **2011**, *99* (3), 914–923.
(32) Politi, R.; Harries, D. Enthalpically driven peptide stabilization by protective osmolytes. *Chem. Commun.* **2010**, *46* (35), 6449–6451.
(33) Maynard, A. J.; Sharman, G. J.; Searle, M. S. Origin of beta-hairpin stability in solution: Structural and thermodynamic analysis of the folding of model peptide supports hydrophobic stabilization in water. *J. Am. Chem. Soc.* **1998**, *120* (9), 1996–2007.
(34) Soper, A. K.; Bruni, F.; Ricci, M. A. Site-site pair correlation functions of water from 25 to 400 degrees C: Revised analysis of new and old diffraction data. *J. Chem. Phys.* **1997**, *106* (1), 247–254.
(35) Mark, P.; Nilsson, L. Structure and dynamics of the TIP3P, SPC, and SPC/E water models at 298 K. *J. Phys. Chem. A* **2001**, *105* (43), 9954–9960.
(36) Auton, M.; Bolen, D. W. Predicting the energetics of osmolyte-induced protein folding/unfolding. *Proc. Natl. Acad. Sci. U. S. A.* **2005**, *102* (42), 15065–15068.
(37) Courtenay, E. S.; Capp, M. W.; Anderson, C. F.; Record, M. T. Vapor pressure osmometry studies of osmolyte-protein interactions: Implications for the action of osmoprotectants in vivo and for the interpretation of "osmotic stress" experiments in vitro. *Biochemistry* **2000**, *39* (15), 4455–4471.
(38) Ghosh, T.; Kalra, A.; Garde, S. On the salt-induced stabilization of pair and many-body hydrophobic interactions. *J. Phys. Chem. B* **2005**, *109* (1), 642–651.
(39) Shukla, D.; Shinde, C.; Trout, B. L. Molecular Computations of Preferential Interaction Coefficients of Proteins. *J. Phys. Chem. B* **2009**, *113* (37), 12546–12554.
(40) Ploetz, E. A.; Bentenitis, N.; Smith, P. E. Developing force fields from the microscopic structure of solutions. *Fluid Phase Equilib.* **2010**, *290* (1−2), 43–47.
(41) Fersht, A. R. *Structure and Mechanism in Protein Science*; 3rd ed.; Palgrave Macmillan U. K.; W. H. Freeman: New York, 1999.
(42) Harries, D.; Rosgen, J. A practical guide on how osmolytes modulate macromolecular properties. In *Biophysical Tools for Biologists: Vol 1 in Vitro Techniques*; Correia, J. J., Detrich, H. W., Eds.; Elsevier: New York, 2008; Vol. 84, pp 679.
(43) Auton, M.; Bolen, D. W. Application of the transfer model to understand how naturally occuring osmolytes affect protein stability. *Osmosensing Osmosignaling* **2007**, *428*, 397–418.
(44) Luzar, A.; Chandler, D. Effect of environment on hydrogen bond dynamics in liquid water. *Phys. Rev. Lett.* **1996**, *76* (6), 928–931.
(45) Kumar, R.; Schmidt, J. R.; Skinner, J. L. Hydrogen bonding definitions and dynamics in liquid water. *J. Chem. Phys.* **2007**, *126*, 20.
(46) Politi, R.; Sapir, L.; Harries, D. The Impact of Polyols on Water Structure in Solution: A Computational Study. *J. Phys. Chem. A* **2009**, *113* (26), 7548–7555.
(47) McDonald, I. K.; Thornton, J. M. Satisfying Hydrogen-Bonding Potential in Proteins. *J. Mol. Biol.* **1994**, *238* (5), 777–793.
(48) Espinosa, E.; Molins, E.; Lecomte, C. Hydrogen bond strengths revealed by topological analyses of experimentally observed electron densities. *Chem. Phys. Lett.* **1998**, *285* (3−4), 170–173.
(49) Arnold, W. D.; Sanders, L. K.; McMahon, M. T.; Volkov, R. V.; Wu, G.; Coppens, P.; Wilson, S. R.; Godbout, N.; Oldfield, E. Experimental, Hartree-Fock, and density functional theory investigations of the charge density, dipole moment, electrostatic potential, and electric field gradients in L-asparagine monohydrate. *J. Am. Chem. Soc.* **2000**, *122* (19), 4708–4717.
(50) Galvez, O.; Gomez, P. C.; Pacios, L. F. Variation with the intermolecular distance of properties dependent on the electron density in hydrogen bond dimers. *J. Chem. Phys.* **2001**, *115* (24), 11166–11184.
(51) Stumpe, M. C.; Grubmuller, H. Aqueous urea solutions: Structure, energetics, and urea aggregation. *J. Phys. Chem. B* **2007**, *111* (22), 6220–6228.
(52) Lee, S. L.; Debenedetti, P. G.; Errington, J. R. A computational study of hydration, solution structure, and dynamics in dilute carbohydrate solutions. *J. Chem. Phys.* **2005**, *122*, 20.
(53) Czapiewski, D.; Zielkiewicz, J. Structural Properties of Hydration Shell Around Various Conformations of Simple Polypeptides. *J. Phys. Chem. B* **2010**, *114* (13), 4536–4550.
(54) Jaynes, E. T. Information Theory and Statistical Mechanics. *Phys. Rev.* **1957**, *106* (4), 620–630.
(55) Zielkiewicz, J. Two-particle entropy and structural ordering in liquid water. *J. Phys. Chem. B* **2008**, *112* (26), 7810–7815.
(56) Griffiths-Jones, S. R.; Maynard, A. J.; Searle, M. S. Dissecting the stability of a beta-hairpin peptide that folds in water: NMR and molecular dynamics analysis of the beta-turn and beta-strand contributions to folding. *J. Mol. Biol.* **1999**, *292* (5), 1051–1069.
(57) Searle, M. S.; Griffiths-Jones, S. R.; Skinner-Smith, H. Energetics of weak interactions in a beta-hairpin peptide: Electrostatic and hydrophobic contributions to stability from lysine salt bridges. *J. Am. Chem. Soc.* **1999**, *121* (50), 11615–11620.
(58) Paul, S.; Patey, G. N. Structure and interaction in aqueous urea-trimethylamine-N-oxide solutions. *J. Am. Chem. Soc.* **2007**, *129* (14), 4476–4482.
(59) Zhang, Y. J.; Cremer, P. S. Chemistry of hofmeister anions and osmolytes. In *Annu. Rev. Phys. Chem.*; Leone, S. R., Cremer, P. S., Groves, J. T., Johnson, M. A., Richmond, G., Eds.; Annual Reviews: Palo Alto, CA, 2010; Vol. 61.
(60) Canchi, D. R.; Garcia, A. E. Backbone and Side-Chain Contributions in Protein Denaturation by Urea. *Biophys. J.* **2011**, *100* (6), 1526–1533.
(61) Hu, C. Y.; Lynch, G. C.; Kokubo, H.; Pettitt, B. M. Trimethylamine N-oxide influence on the backbone of proteins: An oligoglycine model. *Proteins: Struct. Funct. Bioinf.* **2010**, *78* (3), 695–704.
(62) Blackburn, G. M.; Lilley, T. H.; Walmsley, E. Aqueous-Solutions Containing Amino-Acids and Peptides. 13. Enthalpy of Dilution and Osmotic Coefficients of Some N-Acetyl Amino-Acid Amides and Some N-Acetyl Peptide Amides at 298.15 K. *J. Chem. Soc., Faraday Trans. I* **1982**, *78*, 1641–1665.
(63) Gaffney, S. H.; Haslam, E.; Lilley, T. H.; Ward, T. R. Homotactic and Heterotactic Interactions in Aqueous-Solutions Containing Some Saccharides - Experimental Results and an Empirical Relationship between Saccharide Solvation and Solute Solute Interactions. *J. Chem. Soc., Faraday Trans. I* **1988**, *84*, 2545–2552.
(64) Li, L.; Zhu, L. Y.; Qiu, X. M.; Sun, D. Z.; Di, Y. Y. Concentration effect of sodium chloride on enthalpic interaction coefficients of D-mannitol and D-sorbitol in aqueous solution. *J. Therm. Anal. Calorim.* **2007**, *89* (1), 295–301.
(65) Collins, K. D.; Washabaugh, M. W. The Hofmeister effect and the behaviour of water at interfaces. *Q. Rev. Biophys.* **1985**, *18* (4), 323–422.
(66) de Gennes, P.-G. *Scaling Concepts in Polymer Physics*; Cornell University Press: Ithaca, NY, 1979; p 315.
(67) Rubinstein, M.; Colby, R. H. *Polymer Physics*; Oxford University Press: Oxford, U. K., 2003; p 440.
(68) Ferreon, J. C.; Ferreon, A. C. M.; Bolen, D. W.; Hilser, V. J. Discrepancy between conformational stabilities obtained from native state hydrogen-deuterium exchange and denaturant-induced unfolding. *Biophys. J.* **2003**, *13* (2), 84A−13A.
(69) Asakura, S.; Oosawa, F. On Interaction between Two Bodies Immersed in a Solution of Macromolecules. *J. Chem. Phys.* **1954**, *22*, 1255–1256.
(70) Knowles, D. B.; LaCroix, A. S.; Deines, N. F.; Shkel, I.; Record, M. T. Separation of preferential interaction and excluded volume effects on DNA duplex and hairpin stability. *Proc. Natl. Acad. Sci. U. S. A.* **2011**, *108* (31), 12699–12704.
(71) Phillips, J. C.; Braun, R.; Wang, W.; Gumbart, J.; Tajkhorshid, E.; Villa, E.; Chipot, C.; Skeel, R. D.; Kale, L.; Schulten, K. Scalable molecular dynamics with NAMD. *J. Comput. Chem.* **2005**, *26* (16), 1781–1802.
(72) Brooks, B. R.; Bruccoleri, R. E.; Olafson, B. D.; States, D. J.; Swaminathan, S.; Karplus, M. Charmm - a Program for Macromolecular

Energy, Minimization, and Dynamics Calculations. *J. Comput. Chem.* **1983**, *4* (2), 187–217.

(73) MacKerell, A. D.; Bashford, D.; Bellott, M.; Dunbrack, R. L.; Evanseck, J. D.; Field, M. J.; Fischer, S.; Gao, J.; Guo, H.; Ha, S.; Joseph-McCarthy, D.; Kuchnir, L.; Kuczera, K.; Lau, F. T. K.; Mattos, C.; Michnick, S.; Ngo, T.; Nguyen, D. T.; Prodhom, B.; Reiher, W. E.; Roux, B.; Schlenkrich, M.; Smith, J. C.; Stote, R.; Straub, J.; Watanabe, M.; Wiorkiewicz-Kuczera, J.; Yin, D.; Karplus, M. All-atom empirical potential for molecular modeling and dynamics studies of proteins. *J. Phys. Chem. B* **1998**, *102* (18), 3586–3616.

(74) Humphrey, W.; Dalke, A.; Schulten, K. VMD: Visual molecular dynamics. *J. Mol. Graphics* **1996**, *14* (1), 33–&.

(75) Blodgett, M. B.; Ziemer, S. P.; Brown, B. R.; Niederhauser, T. L.; Woolley, E. M. Apparent molar volumes and apparent molar heat capacities of aqueous adonitol, dulcitol, glycerol, meso-erythritol, myo-inositol, D-sorbitol, and xylitol at temperatures from (278.15 to 368.15) K and at the pressure 0.35 MPa. *J. Chem. Thermodyn.* **2007**, *39* (4), 627–644.

(76) Rosgen, J., Molecular basis of osmolyte effects on protein and metabolites. In *Osmosensing and Osmosignaling*; Elsevier Academic Press Inc: San Diego, CA, 2007; Vol. 428, pp 459−486.

(77) Lazaridis, T.; Paulaitis, M. E. Simulation Studies of the Hydration Entropy of Simple, Hydrophobic Solutes. *J. Phys. Chem.* **1994**, *98* (2), 635–642.

(78) Bergman, D. L.; Lyubartsev, A. P.; Laaksonen, A. Topological and spatial aspects of the hydration of solutes of extreme solvation entropy. *Phys. Rev. E* **1999**, *60* (4), 4482–4495.